Structural Arrangement of Crystalline/Amorphous Phases of Polyethylene-*block*-Polystyrene Copolymer as Induced by Orientation Techniques

Hiroki UEHARA[1*], *Tomoyuki YOSHIDA, Masaki KAKIAGE*[1],

Takeshi YAMANOBE[1], *Tadashi KOMOTO*[1]

[1]Department of Chemistry, Gunma University, Kiryu, Gunma 376-8515, Japan

uehara@chem.gunma-u.ac.jp

ABSTRACT.

Polyethylene-*block*-polystyrene (PE-*block*-PS) copolymer film having bicontinuous crystalline/amorphous phases were tensile-drawn under various conditions for structural arrangement of these phases. When a draw was made below melting temperature of PE crystalline phase (95^{o}C), the bicontinuous structure was gradually destroyed with increasing strain, due to the lower ductility of PS having glass-transition temperature around 100^{o}C. Correspondingly, the necking phenomenon was clearly recognizable during draw. In contrast, a draw near melting temperature of PE crystalline phase gave the less orientation of PE phases, resulting in homogeneous deformation with the lower draw stress. These results indicated that the modification of the lower ductility of PS was required for the effective orientation of these phases. Here, a solvent swelling technique was applied to improve PS deformability even below its glass-transition temperature. Tensile drawing after such treatment could successfully induce the orientation of both crystalline/amorphous phases. A transition from necking to homogenous deformation was also observed in stress/strain behavior.

Keywords: polyethylene, polystyrene, block copolymers, drawing, swelling

MANUSCRIPT TEXT.

Introduction

Generally, the ordered arrangement of separated phases of block copolymer is maintained within each domain having the several-μm size, but divided like mosaic, resulting in the random orientation in the bulk level. The spatial continuity of such ordered arrangement is required for the lithographic application using block copolymer,[1-10] where the thickness limitation within thin film induces the ordered arrangement over the larger area beyond the usual domain size.

Recently, the characteristics of these separated phases are tried to be withdrawn in the bulk state by the homogeneous spreading of their ordered arrangements within the whole bulk size. For preparation of such bulk morphology composed by the homogenous arrangement of the separated phases, various external fields, including force,[11-21] magnetic, and electric fields[9,22-25] have been applied.

In the case of the force field, the shear flow[12-14] and tensile drawing[15-18] are often applied for directionally arrangement of separated phases of block copolymer, where the unique transition from the initial lamellar stacking to the deformed chevron morphology has been reported for polystyrene (PS)-*block*-polyisoprene copolymer. However, the orientation of the separated phases easily relaxes after releasing the applied tensile force, due to its rubbery characteristic. Therefore, it is difficult to obtain the highly oriented morphology of this copolymer. In order to fix the morphological orientation induced by the tensile force, Sakurai *et al.*[11] introduce the cross-linking into the copolymer chains after tensile deformation.

In contrast, the crystallization is also utilized to restrict the relaxation of the oriented morphology after deformation. Loo *et al.*[26-29] oriented the cylinder morphology of the polyethylene (PE)-*block*-PS copolymer by shear flow during melt-extrusion through channel die. The orientation along the extrusion axis could be locked by oriented crystallization of PE block.

In this study, we tried the tensile drawing of PE-*block*-PS copolymer. Tensile drawing is the most effective orientation method for ductile polymeric materials such as PE.[30] In order to resist the higher

tensile force in the solid state, the sample films were prepared from the sample having the higher molecular weight over 10^4. The structural change with tensile deformation was analyzed by a combination of *ex-situ* microscopic and *in-situ* X-ray measurements. The obtained results were compared to the stress-strain behaviors of the samples, giving the discussion on the mechanisms of the structural arrangement induced by tensile force.

Experimental

Initial Materials. The material used was PE-*block*-PS copolymer purchased from Polymer Source Inc. in Quebec, Canada, which is the same as used in our previous study.[31] The number average molecular weight of each component was 5.4×10^4 for PS and 6.7×10^4 for PE, with a molecular weight distribution of 1.04.

Film Preparation. The sample was dissolved into *p*-xylene at its boiling point for 10 min., followed by casting into a Teflon dish and drying at room temperature in a vacuum. The obtained circular film, having a radius of 90 mm and a thickness of 30mm, was melted at 180°C, and then isothermally crystallized at an optimum temperature of 90°C in a vacuum oven for three days.

Drawing. The drawing specimens were cut into a strip with 50 mm length and 5 mm width from the above prepared film. These strips were tensile drawn at constant drawing temperatures (T_d) from room temperature to 90°C and a constant cross-head speed, corresponding to the initial strain rate of 1 min^{-1}, in an Orientec Tensilon tensile tester RTC-1325A equipped with an air oven. The draw ratio (*DR*) was determined from the separation of ink marks preprinted on the surface of samples.

Fuming Nitric Acid Etching. Fuming nitric acid etching of the film was performed at room temperature for 30 min. An excess amount of fuming nitric acid (10 ml) was added to 0.1 g of the sample film in a glass bottle. Following this etching procedure, the treated film was washed with distilled water and then acetone, and dried well at room temperature.

Measurements. Thermal gravimetric analyses (TGA) of the sample films were made by using a Rigaku TG8120. Weight loss during heating at 5°C/min was recorded from room temperature to 500°C.

In-situ small-angle X-ray scattering (SAXS) measurements were carried out during drawing by using a synchrotron radiation source at the BL40B2 beamline of SPring-8 (Japan Synchrotron Radiation Research Institute, Hyogo, Japan). Our extension device was set in the beamline, and WAXD images were continuously recorded during drawing on a cooling-type CCD camera (Hamamatsu Photonics K.K., C4880). The wavelength of the synchrotron beam was 1 angstrom. The exposure time for each pattern was 25 seconds with a time interval of 5 seconds for date storage. The drawing stress was simultaneously recorded by using a load cell (Kyowa Electronic Instruments Co., Ltd., LUR-A-50NSA1) installed in the extension device.

Transmission electron microscopic (TEM) observations of the drawn films were made by a JEOL 1200EMX electron microscope operated at 80 kV. The samples were stained by RuO_4 vapor and embedded in epoxy resin. The assembly was cut into thin sections with 60 nm thick, using a Reichert UltraCut S. microtome for TEM observation. Scanning electron microscope (SEM) observations of the etched samples were made using a Hitachi S-5000 field emission SEM operated at 5 kV. The sample surface was coated by Pt-Pd with 2 nm using a Hitachi ion spatter E-1030.

Results and Discussions

Our previous study[31] revealed that the crystalline/amorphous morphology of the PE-*block*-PS copolymer is controllable by changing the crystallization conditions. Especially, the optimum crystallization temperature of 90^{o}C for the same PE-*block*-PS copolymer as used in this study gave the bicontinuous crystalline/amorphous phase separation, as shown in Figure 1. In this study, we tried to withdraw the higher ductility of PE component to prepare the ordered arrangement of these phases by applying various orientation techniques.

As the first trial, the tensile drawing under various T_ds was carried out for the film isothermally crystallized at 90^{o}C. Here, a DSC thermogram of this film (not shown here) exhibited the endotherm attributed to the melting of PE crystalline component around 95^{o}C, thus the T_ds in this study were selected at 90^{o}C just below melting peak and room temperature. A T_d = 60^{o}C in the middle range of

these temperatures was also adopted. Figure 2 shows the stress-strain curve recorded under these T_ds. With increasing T_d, the drawing stress decreases, but the necking was always observed in the lower strain region, independent of T_d. Beyond this necking, the strain-hardening occurs at T_ds of room temperature and 60°C. In contrast, such stress increasing was not recognized at a T_d of 90°C. These results indicate that the deformation of PE component proceeds in the partially molten state at this higher T_d. Among these three T_ds, a T_d of 60°C gave the highest resultant *DR*, as shown in Figure 2.

The phase arrangements of these drawn films were analyzed by TEM observations. Figure 3 shows the drawn morphologies obtained under various conditions. As compared to initial morphology before drawing (see Figure 1), the continuity of the crystalline/amorphous phases is lost at both T_ds of room temperature and 90°C, but the characteristic morphology like chevron[12-18] is observed at a T_d of 60°C. Therefore, a further drawing was made at 60°C up to the higher *DR* of 3 (see Figure 3 (d)), but the phase continuity was destroyed as similar to those obtained at T_ds of room temperature and 90°C. This is ascribed to the lower ductility of PS component below its glass-transition temperature (T_g), which is also indicated by the stress increasing at the later stage of draw as shown in Figure 2 (a). The higher T_d over 90°C gave an ineffective draw, leading to the sample breaking at the initial stage of drawing.

These results suggest that an improvement of the ductility of PS component is required even below its T_g for the ordered arrangement of these crystalline/amorphous phases. Here, we paid our attentions to the difference of the solubility of PE and PS. For example, PS is soluble in toluene even at room temperature, but PE is insoluble. If the PS component is swelled and softened by toluene, the drawing at the lower T_d becomes possible, giving the effective phase arrangement. Therefore, the film isothermally crystallized at 90°C was swelled in toluene for 1 min and subsequently held under atmosphere at room temperature for 10 min. Figure 4 compares the TGA curves of such swelled film and the untreated film. For the swelled film, the 7% weight loss was observed around 110°C, corresponding to the boiling point of toluene. This means that toluene is still contained in the swelled film even after holding under an ambient condition for 10 min. Such residual toluene increases the PS volume but the initial continuity of

the crystalline/amorphous phases are maintained even after solvent swelling, as shown in the TEM image of Figure 5.

The effect of such a solvent swelling on the stress-strain behavior was discussed first. Figure 6 (a) and (b) compares the stress-strain curves recorded before and after solvent swelling treatment for the film isothermally crystallized at 90^{o}C. Also, the data for the film prepared by quenching from the melt without solvent swelling were depicted in Figure 6 (c). For the melt-quenched film, the drawing stress was lower than that for the film isothermally crystallized at 90^{o}C, due to the less developed continuity of the crystalline phases. However, the drawing stress of the solvent-swelled film is further lowered, as shown in (b). Additionally, the necking phenomena are observed in the lower strain region for the former two films, but not recognized for the latter. These features in the stress-strain behaviors imply that the ductility improvement of PS component by the selective solvent swelling induces an effective orientation of both crystalline/amorphous phases by tensile drawing.

Therefore, the morphologies of the films drawn after solvent swelling treatment were analyzed by a combination of TEM and SEM observations. For TEM observation, the amorphous region was selectively stained by RuO_4, which appears as the darker region in the image. In contrast, the amorphous region was selectively removed by acid etching for SEM observations to emphasize the crystalline region. Such an etching procedure has been often applied for analyzing the drawn morphologies of PE homopolymer.[32] Figure 7 shows TEM (top) and SEM (bottom) images for the film swelled by toluene, subsequently drawn at room temperature up to *DR*s of 1.6 (left) and 3.2 (right). The initial films were isothermally crystallized at 90^{o}C. These images exhibit the gradual orientation of the cylinder along the drawing axis with increasing *DR*. The continuity of the crystalline/amorphous phases looks maintained even after draw, as compared to those of the films drawn without solvent swelling treatment (see Figure 3). In summery, a solvent swelling procedure transforms the PS component from brittle to ductile even below its T_g, which enables an effective drawing of both crystalline/amorphous phases with keeping their bicontinuities.

In the cases of TEM and SEM observations, the sizes of these phases are determinable but the sampling areas are limited within the magnified field. Therefore, these observation techniques are not preferred for the size analysis of the focused structure. In contrast, the scattering analysis replies the average value for the larger area. Additionally, the latter analysis is sometimes applicable as *in-situ* method, which well corresponds to the stress-strain measurements shown in Figure 6. Such *in-situ* measurement requires the higher time-resolution to detect the analyzable data, having enough S/N for analysis, within the shorter time scale. In this study, the SAXS measurements using strong synchrotron radiation source were adopted. The *in-situ* SAXS patterns recorded during tensile drawing of the films with or without solvent swelling treatment, and the obtained results were compared. Figures 8 and 9 show the stress-strain curves of the untreated and solvent-treated films and the corresponding changes in the *in-situ* SAXS patterns recorded during drawing at room temperature. For both films, the pattern transforms from the ring to the ellipse with drawing, indicating that the crystalline/amorphous phases orient along the draw axis. At the later stage of the drawing, the four-point patterns were observed. However, the differences in these pattern changes in Figures 8 and 9 are not obvious. Thus, quantitative analyses of these structural changes were made by comparing the line profiles extracted along the equators from the series of *in-situ* SAXS patterns. The obtained equatorial line profiles for the untreated and solvent-treated film were plotted as a function of drawing strain in Figure 10 (a) and (b), respectively. The beam stopper cuts the lower 2θ region below 0.1degree. When the long period at 50% strain was compared, those of the untreated and solvent-treated film were 55 nm and 63 nm, respectively. The higher long period of the solvent-treated film at the same stain is attributed to the initial volume increase of PS component before drawing, as indicated the TEM image shown in Figure 5. During drawing the untreated film, the position of long period peak gradually shifts into the higher 2θ, but disappeared at the later stage of draw. Considering with the drawn morphologies shown in Figure 3, this means that the continuity of the PS components was destroyed for the untreated film at the higher *DR*. In contrast, the long period peak survives even at the final strain of 230%, leading to the long period value of 40 nm. This indicates that the film treated by toluene was effectively drawn up to the

higher *DR* with keeping the continuity of the both crystalline/amorphous phases, which is well coincident to the morphological analysis shown in Figure 7.

Conclusions

The oriented arrangement of the bicontinuous crystalline/amorphous morphology of PE-*block*-PS copolymer film was prepared by applying drawing technique. The tensile drawing below the melting temperature for PE component (95^{o}C) destroys the initial continuity of PS component with increasing strain, due to the higher T_g of 100^{o}C for PS component. Correspondingly, the obvious necking occurs during drawing below these critical temperatures. We consider that the ductility of PS component is necessarily improved for enabling the oriented arrangement of both bicontinuous components. The swelling by toluene plasticizes the PS component even below its T_g. As a result, both components could be arranged by tensile drawing with keeping their continuities. Such a solvent swelling also reduced the drawing stress, leading to the transition from necking deformation to homogeneous deformation.

ACKNOWLEDGMENT.

In-situ WAXD measurement used synchrotron radiation was performed in SPring-8, Japan Synchrotron Radiation Research Institute (2005A0699-NL2b-np). Experimental support is gratefully acknowledged.

FIGURE CAPTIONS.

Figure 1. TEM image of the initial morphology of the films used in this study. Scale bar, 250nm. The as-cast film of PE-*block*-PS was melted at 180^{o}C, and isothermally crystallized at 90^{o}C for 3 days.

Figure 2. Stress-strain curves of the films isothermally crystallized at 90^{o}C. Tensile tests were made at different T_ds of room temperature (a), 60^{o}C (b), and 90^{o}C (c).

Figure 3. TEM images of the films drawn under various conditions. (a) T_d = room temperature, *DR* = 2.4; (b) T_d =60^{o}C, *DR* = 2.5;(c) T_d = 90^{o}C, *DR* = 3.3; (d) T_d = 60^{o}C, *DR* = 3.0.

Figure 4. Comparison of TGA curves recorded for the film isothermally crystallized at 90^{o}C (a) and after solvent swelling treatment (b). Heating rate was 5^{o}C/min.

Figure 5. Morphological change induced by solvent swelling treatment. (a) Before and (b) after treatment. Scale bar, 250nm. Corresponding enlarged images were also attached on left bottom side. Scale bar, 50nm.

Figure 6. Change in stress/strain behavior after solvent swelling treatment. (a) Before and (b) after treatment for the film isothermally crystallized at 90^{o}C. For comparison, the curve recorded for the film prepared by quenching from the melt was also included. Tensile tests were made at room temperature.

Figure 7. Drawn morphologies obtained after solvent swelling treatment. Left and right sets were observed for the film drawn at room temperature up to *DR* = 1.6 (a, c) and up to *DR* = 3.2 (b, d), respectively. Top and bottom sets show internal (TEM) and surface morphologies after acid etching (SEM). Scale bar, 150nm.

Figure 8. Stress profile recorded at room temperature with corresponding change of *in-situ* SAXS patterns during drawing of the initial dried film. The draw direction for the SAXS patterns is horizontal. The strain in percent is indicated for each pattern. Drawing was applied within the time region sandwiched between two dashed lines.

Figure 9. Stress profile recorded at room temperature with corresponding change of *in-situ* SAXS patterns during drawing of the film swelled by toluene. The meanings of the other marks are the same as shown in Figure 8.

Figure 10. Comparison of the line profiles extracted along the equators of the series of *in-situ* SAXS patterns recorded during drawing of the initial (a) and swelled films (b).

REFERENCES.

1. Park, M.; Harrison, C.; Chaikin, P. M.; Register, R. A.; Adamson, D. H. Science 1997, 276, 1401-1404.

2. Thurn-Albrecht, T.; Schotter, J.; Kastle, G. A.; Emley, N.; Shibauchi, T.; Krusin-Elbaum, L.; Guarini, K.; Black, C. T.; Tuominen, M. T.; Russell, T. P. Science 2000, 290, 2126-2129.

3. Cheng, J. Y.; Ross, C. A.; Chan, V. Z.-H.; Thomas, E. L.; Lammertink, R. G. H.; Vancso, G. J. Adv. Mater. 2001, 13, 1174-1178.

4. Lopes, W. A.; Jaeger, H. M. Nature 2001, 414, 735-738.

5. Kim, H. C.; Jia, X.; Stafford, C. M.; Kim, D. H.; McCarthy, T. J.; Tuominen, M.; Hawker, C. J.; Russell, T. P. Adv. Mater. 2001, 13, 795-797.

6. Kim, S. O.; Solak, H. H.; Stoykovich, M. P.; Ferrier, N. J.; de Pablo, J. J.; Nealey, P. F. Nature 2003, 424, 411-414.

7. Register, R. A. Nature 2003, 424, 378-379.

8. Morkved, T. L.; Wiltzius, P.; Jaeger, H. M.; Grier, D. G.; Witten, T. A. Appl. Phys. Lett. 1994, 64, 422-424.

9. Morkved, T. L.; Lu, M.; Urbas, A. M.; Ehrichs, E. E.; Jaeger, H. M.; Mansky, P.; Russell, T. P. Science 1996, 273, 931-933.

10. Cheng, J. Y.; Ross, C. A.; Thomas, E. L. Appl. Phys. Lett. 2002, 81, 3657-3659.

11. Sakurai, S.; Aida, S.; Okamoto, S.; Ono, T.; Imaizumi, K.; Nomura, S. Macromolecules 2001, 34, 3672-3678.

12. Polis, D. L.; Winey, K. I. Macromolecules 1996, 29, 8180-8187.

13. Polis, D. L.; Winey, K. I. Macromolecules 1998, 31, 3617-3625.

14. Qiao, L.; Ryan, A. J.; Winey, K. I. Macromolecules 2002, 35, 3596-3600.

15. Hermel, T. J.; Hahn, S. F.; Chaffin, K. A.; Gerberich, W. W.; Bates, F. S. Macromolecules 2003, 36, 2190-2193.

16. Ha, Y.-H.; Thomas, E. L. Macromolecules 2002, 35, 4419-4428.

17. Honeker, C. C.; Thomas, E. L. Macromolecules 2000, 33, 9407-9417.

18. Cohen, Y.; Albalak, R. J.; Dair, B. J.; Capel, M. S.; Thomas, E. L. Macromolecules 2000, 33, 6502-6516.

19. Hong, S.; Yang, L.; MacKnight. W. J.; Gido, S. P. Macromolecules 2001, 34, 7009-.7016

20. Hong, S.; Bushelman, A. A.; MacKnight, W. J.; Gido, S. P.; Lohse, D. J.; Fetters, L. J. Polymer 2001, 42, 5909-5914.

21. Albalak, R. J.; Thomas, E. L. J. Polym. Sci., Polym. Phys. 1994, 32, 341-350.

22. Xu, T.; Hawker, C. J.; Russell, T. P. Macromolecules 2003, 36, 6178-6182.

23. Amundson, K.; Helfand, E.; Davis, D. D.; Quan, X.; Patel, S. S.; Smith, S. D. Macromolecules 1991, 24, 6546-6548.

24. Amundson, K;. Helfand, E.; Quan, X.; Smith, S. D. Macromolecules 1993, 26, 2698-2703.

25. Amundson, K.; Helfand, E.; Quan, X.; Hudson, S. D.; Smith, S. D. Macromolecules 1994, 27, 6559-6570

26. Loo, Y.-L.; Register, R. A.; Adamson, D. H. Macromolecules 2000, 33, 8361-8366.

27. Loo, Y.-L.; Register, R. A.; Ryan, A. J. Macromolecules 2002, 35, 2365-2374.

28. Loo, Y.-L.; Register, R. A.; Ryan, A. J; Dee, G. T. Macromolecules 2001, 34, 8968-8977.

29. Loo, Y.-L.; Register, R. A.; Adamson, D. H. J. Polym. Sci., Polym. Phys. 2000, 38, 2564.

30. Zachariardes, A. E.; Porter, R. S. High Modulus Polymers, Marcel Dekker, New York, 1988.

31. Uehara, T.; Yoshida, T.; Kakiage, M.; Yamanobe, T.; Komoto, T.; Nomura, K.; Nakajima, K.; Matsuda, M. submitted.

32. Nakae, M.; Uehara, H.; Kanamoto, T.; Zachariades, A. E.; Porter, R. S. Macromolecules 2000, 33, 2632-2641.

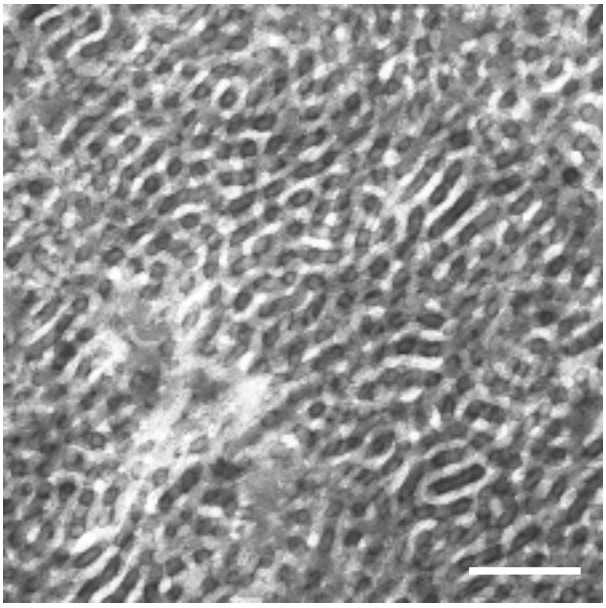

Figure 1 Uehara et al.

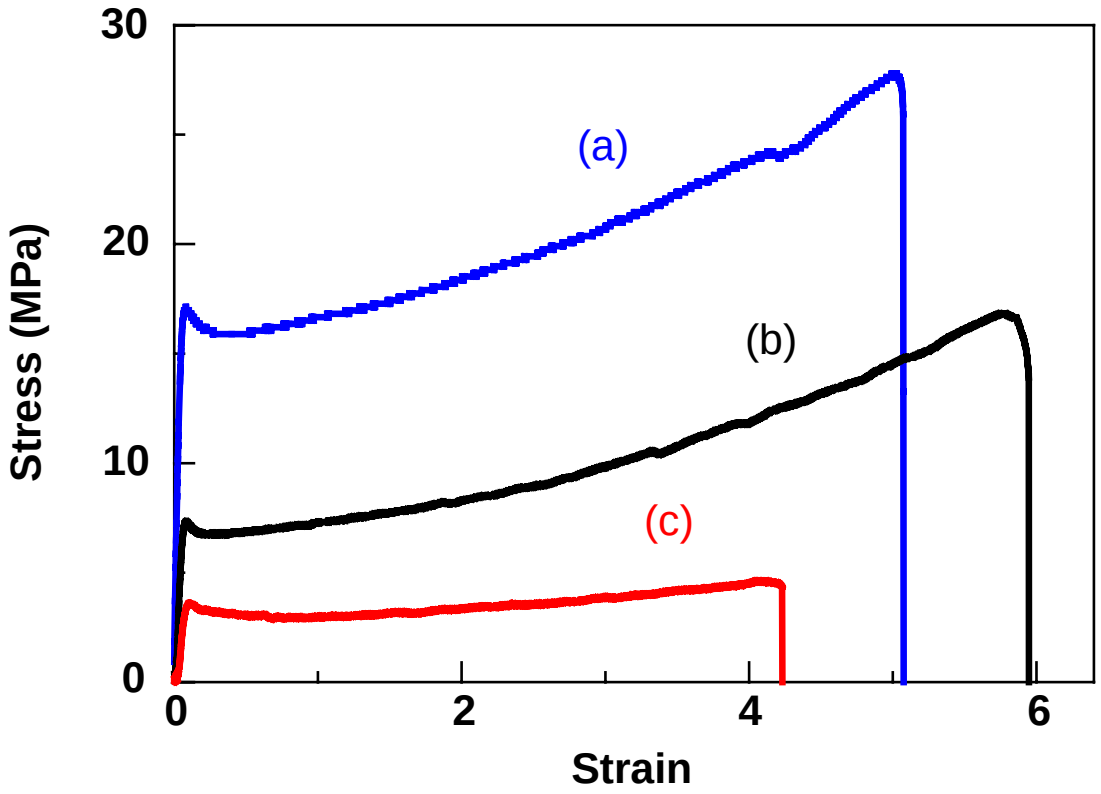

Figure 2 Uehara et al.

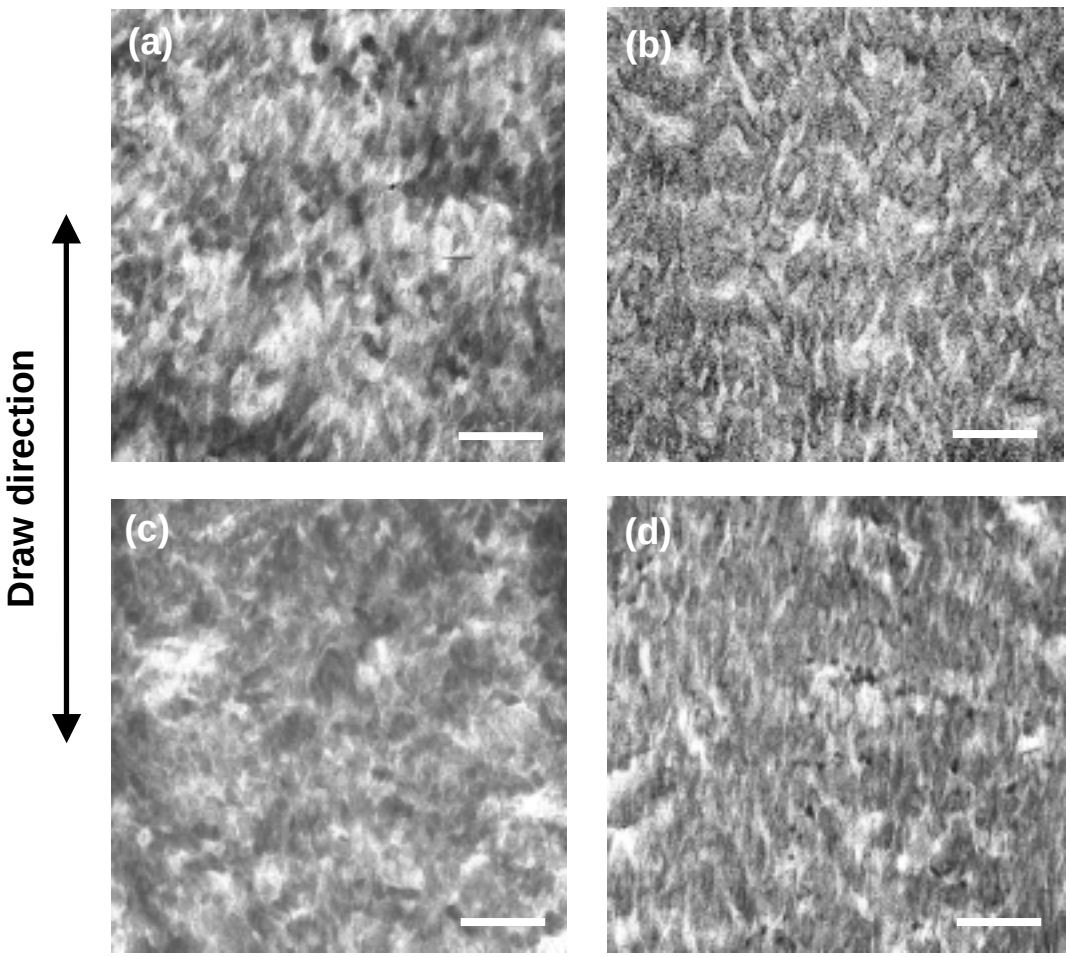

Figure 3 Uehara et al.

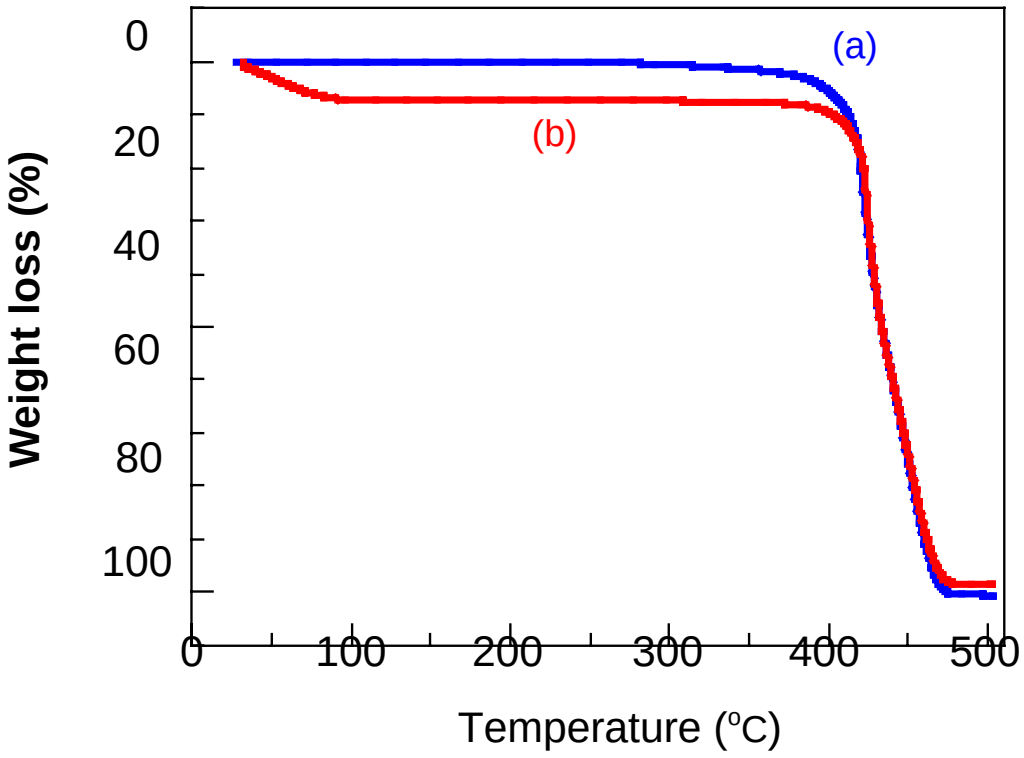

Figure 4 Uehara et al.

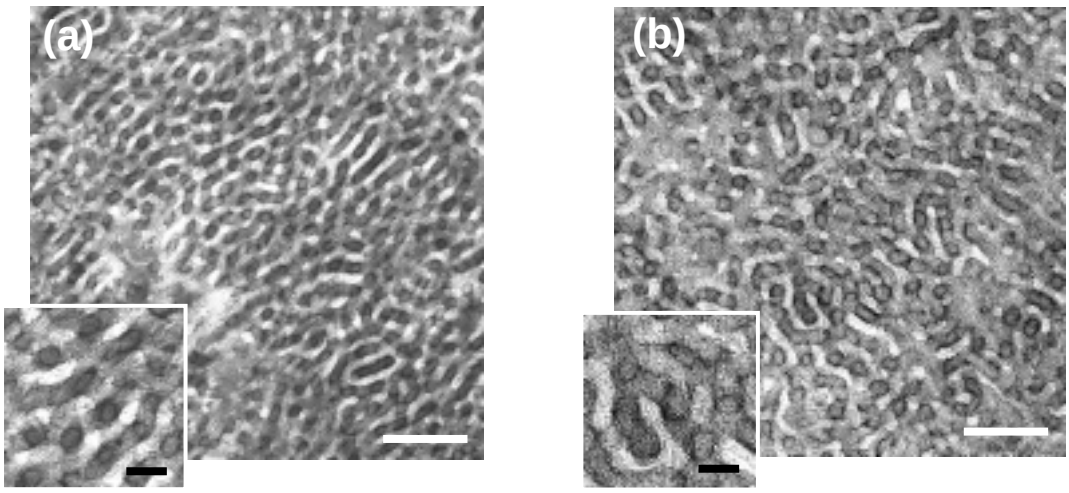

Figure 5 Uehara et al.

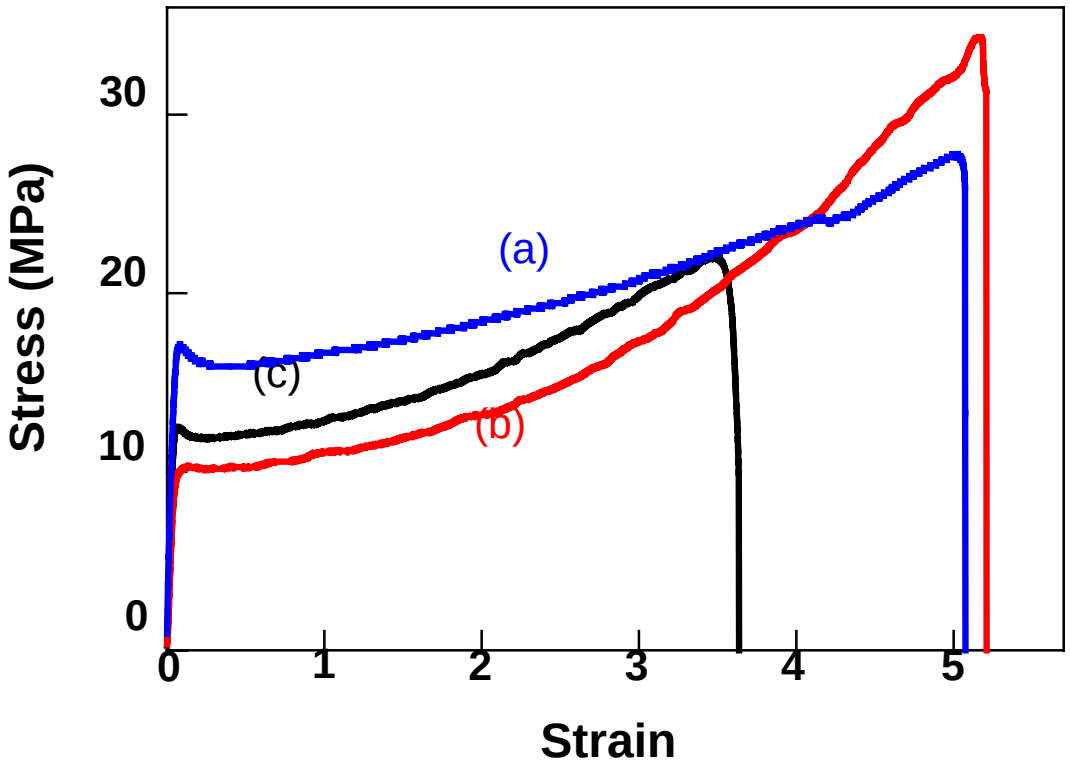

Figure 6 Uehara et al.

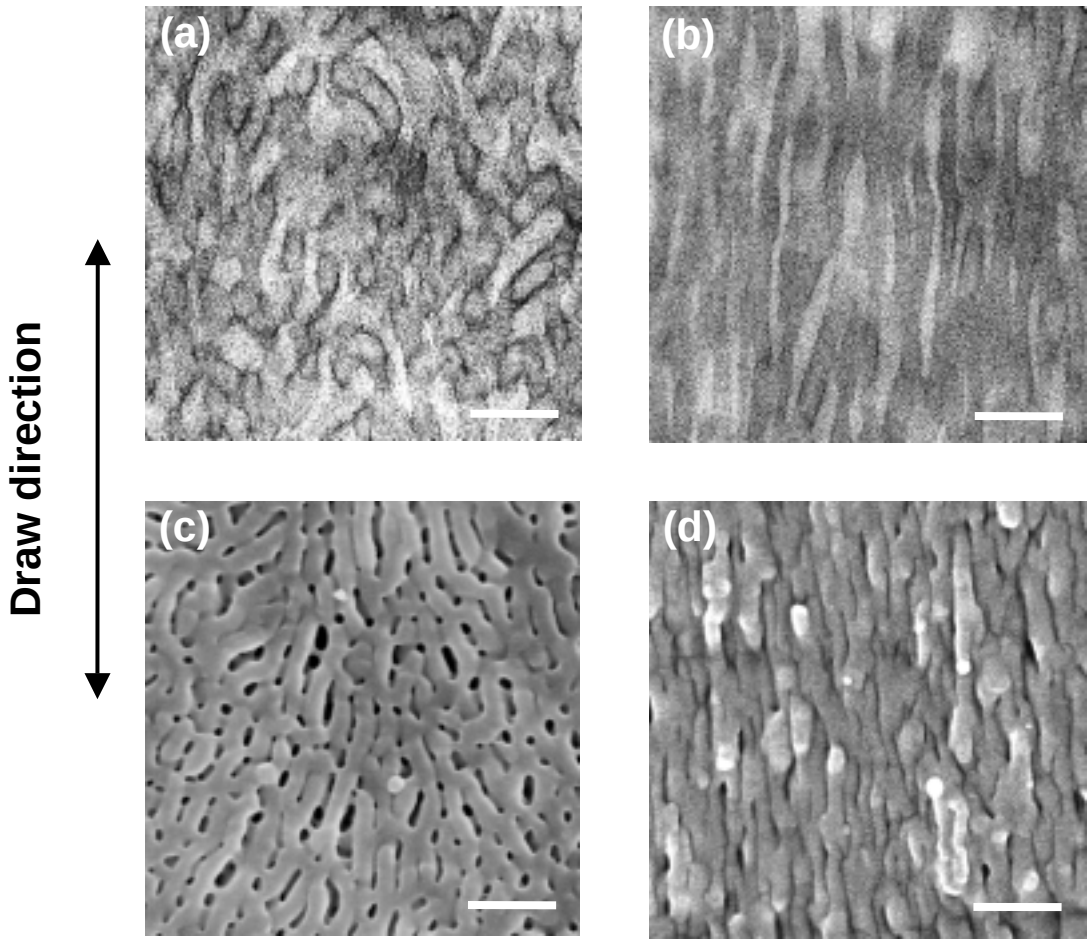

Figure 7 Uehara et al.

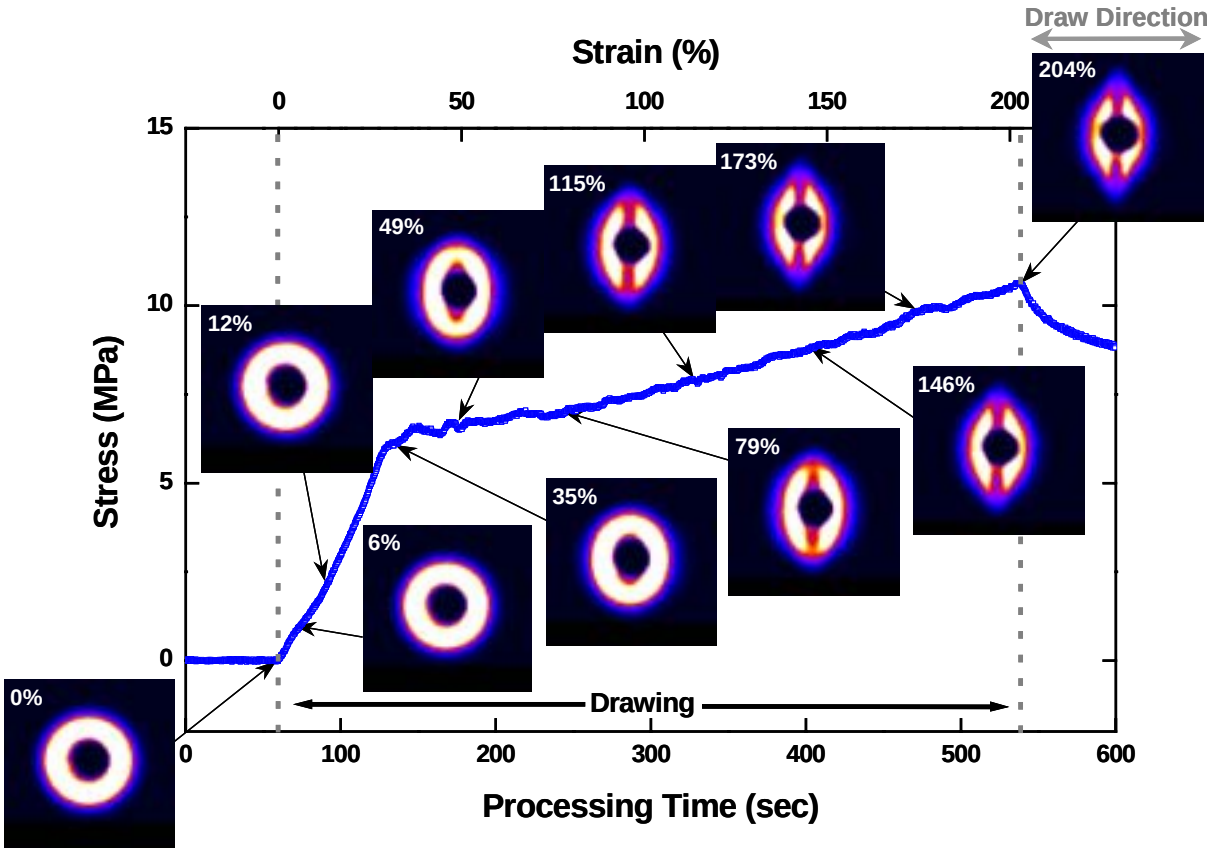

Figure 8 Uehara et al.

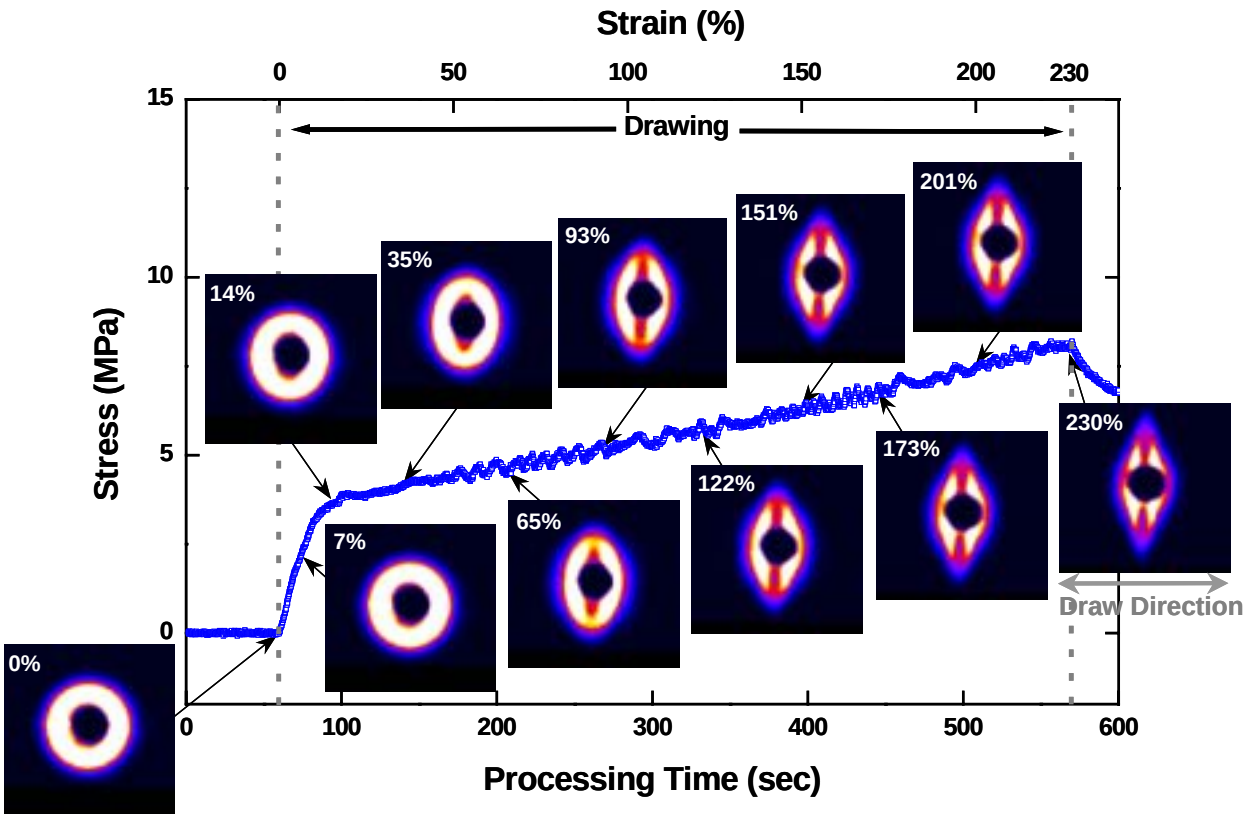

Figure 9 Uehara et al.

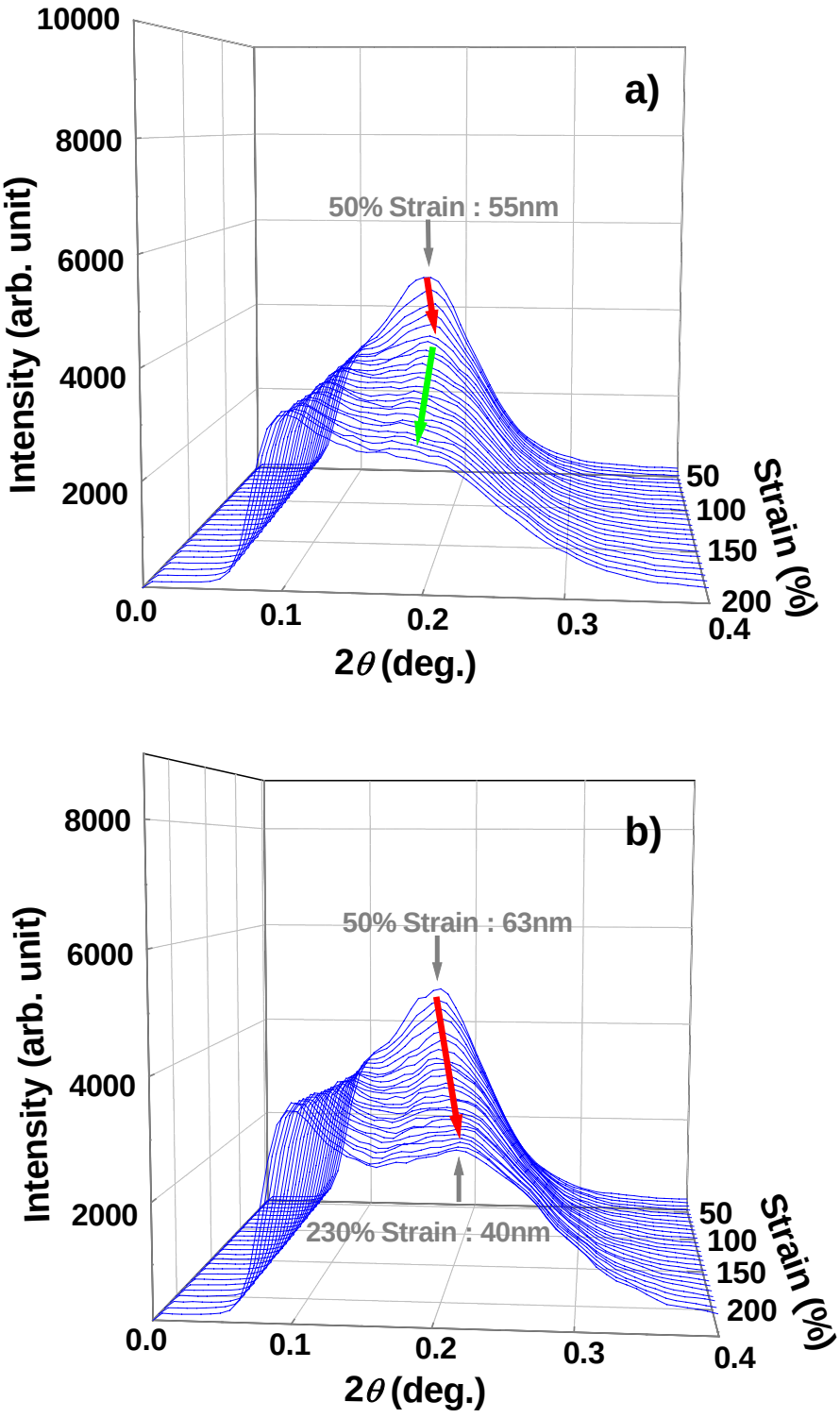

Figure 10 Uehara et al.

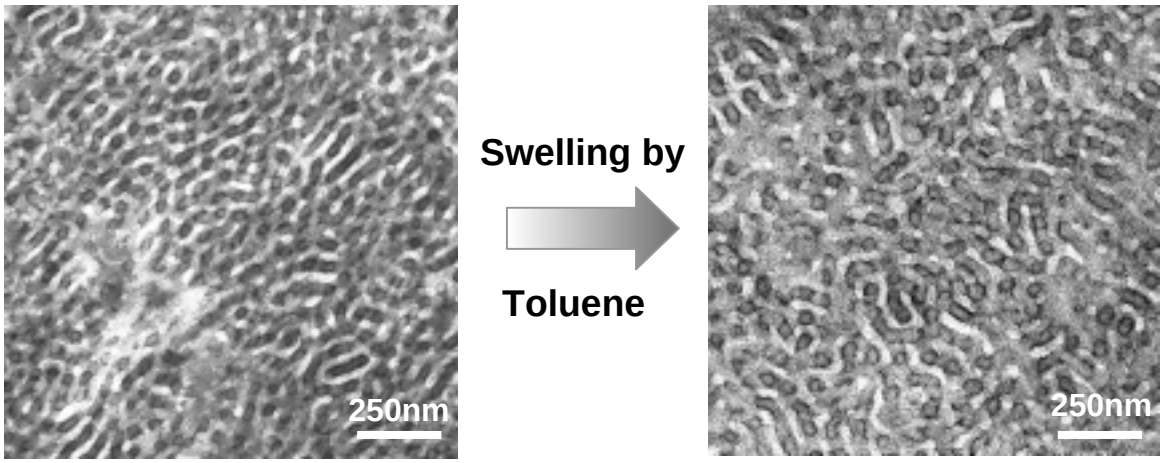

Cover Illustration Uehara et al.